PROCEEDINGS OF THE THIRTEENTH LUNAR AND PLANETARY SCIENCE CONFERENCE, PART 2
JOURNAL OF GEOPHYSICAL RESEARCH, VOL. 88, SUPPLEMENT, PAGES A741-A754, FEBRUARY 15, 1983

NATURE OF THE H CHONDRITE PARENT BODY REGOLITH: EVIDENCE FROM THE DIMMITT BRECCIA

Alan E. Rubin*, Edward R. D. Scott, G. Jeffrey Taylor,
Klaus Keil and Jaclyn S. B. Allen

Department of Geology and Institute of Meteoritics
University of New Mexico, Albuquerque, New Mexico 87131

T. K. Mayeda and R. N. Clayton

Enrico Fermi Institute, University of Chicago, Chicago, Illinois 60637

D. D. Bogard

Geochemistry Branch, Johnson Space Center, Houston, Texas 77058

Abstract. The Dimmitt H chondrite regolith breccia consists of (in vol.%) 40% H4 and H5 chondrite clasts, 3% impact melt rock clasts, 0.5% shocked H chondrite clasts, 1.5% exotic clasts (including carbonaceous and LL5 chondrites), and 55% gas-rich matrix. The LL5 clast is the best documented example of an ordinary chondrite in a host of a different compositional group. The matrix contains unequilibrated material, which differs from typical H3 material in having little (0.2 vol.%) fine-grained opaque silicate matrix, and having 20% of the olivines with compositions in the range Fa_{21-24}. About 10-15% of this unequilibrated material is probably derived from graphite-magnetite-rich chondrites and 2% from H3.0-3.5 chondrites. The absence of H3 clasts suggests that most of the unequilibrated material was derived from unconsolidated type 3 components. Many exotic clasts may have been derived from planetesimals that accreted to the H chondrite parent body prior to regolith development. One slowly cooled melt rock clast formed beneath a 500-m-thick melt breccia pile on the floor of a large impact crater and was later excavated by additional impacts, incorporated into the regolith and consolidated with other components to form the Dimmitt breccia.

Introduction

Meteorite regolith breccias are clastic rocks that formed by lithification of fragmental regolith material that once resided at the surface of a meteorite parent body. These breccias are characterized by solar wind-implanted rare gases [Suess et al., 1964], solar flare particle tracks [Pellas et al., 1969], impact-melted clasts of regolith material [e.g., Fodor and Keil, 1973], exotic clasts, i.e., materials not found in unbrecciated meteorites of the same chemical group as the predominant breccia lithology (e.g., carbonaceous chondrite clasts in ordinary chondrite breccias; Wasson and Wetherill, 1979), and a light/dark structure [e.g., Konig et al., 1961]. Because lunar regolith breccias contain the same constituents as the unconsolidated lunar regolith [e.g., Taylor, 1982], meteorite regolith breccias are probably representative samples of the parent body regoliths from which they were derived.

Most previous petrologic studies of H chondrite regolith breccias focused on the large prominent clasts [e.g., Fodor and Keil, 1976; Fodor et al., 1976; Keil and Fodor, 1980; Keil et al., 1980]. Here we report a study of the matrix and 21 clasts of various sizes (0.2-24 mm) in the Dimmitt H chondrite regolith breccia using petrographic and electron microprobe techniques. In addition, oxygen isotope studies of three clasts (DT1, DT3, and DT4) and instrumental neutron activation analysis (INAA) and $^{39}Ar/^{40}Ar$ age dating of one clast (DT4) are reported.

The Dimmitt meteorite (consisting of at least 21 stones with a total weight of 13.5 kg) was found about 1942 near Dimmitt, Texas [Hey, 1966; Hutchison et al., 1977]. Rare gas studies of the dark portions of Dimmitt indicate enrichment in solar-type rare gases [Eberhardt et al., 1966].

Analytical Procedures

Polished and unpolished slabs of Dimmitt (Table 1) (total area 300 cm^2) were examined visually; polished slabs were also viewed microscopically in reflected light. Polished thin sections of clasts and areas of the clastic matrix were examined microscopically, in transmitted and reflected light. During these studies, many smaller clasts (< 1 mm) were identified and also studied. Metallic Fe,Ni grains were etched with a dilute solution of nitric acid in alcohol to bring out structural details. Modal analyses were made in transmitted and reflected light on a Zeiss Universal petrographic microscope.

All clasts (Table 1) and areas of the clastic matrix were analyzed by an electron microprobe; mineral analyses were made using crystal spectrometers, following standard Bence-Albee and ZAF correction procedures [e.g., Fodor and Keil, 1976; Keil, 1967]. Analyses of Fe,Ni for Co were corrected for Co interference from the K_β peak of Fe. Major, minor, and trace element contents of DT4 (the largest clast) were determined by M.-S. Ma and R. A. Schmitt (Oregon State University) by

---

[*] Now at Department of Mineral Sciences, National Museum of Natural History, Smithsonian Institution, Washington, D.C. 20560

Paper number 2B1421.
0148-0227/83/002B-1421$05.00

TABLE 1. Descriptions and Locations of Clasts in the Dimmitt H Chondrite Regolith Breccia

Clast	Area of Dimmitt*	Section	Clast Type	Clast Diameter (mm)
DT1	USNM 1595	USNM 1595	Type 3 chondrite with G-M$^+$ matrix	5
DT2	UNM C10.7	UNM 523	Type 3 chondrite with G-M$^+$ matrix	1
DT3	UNM C10.6a,2	UNM 526	LL5 chondrite	14
DT4	UNM C10.6 UNM C10.9	UNM 467-470;489	Poikilitic melt-rock	24
DT5	UNM C10.3f	UNM 548	H4 chondrite	10 x 25
DT6	UNM C10.8	UNM 532	H5 chondrite	15
DT7	UNM C10.8	UNM 526	Shocked H chondrite	0.9
DT8	UNM C10.9e	UNM 547	Carbonaceous chondrite	3
DT9	UNM C10.3c	UNM 287	Melt-rock with relict debris	5
DT10	UNM C10.5	UNM 525	Melt-rock with relict debris	3
DT11	UNM C10.7	UNM 523	Melt-rock with relict debris	3
DT12	UNM C10.9e	UNM 547	Porphyritic olivine-pyroxene	3 x 4
DT13	UNM C10.8	UNM 532	Porphyritic olivine	6
DT14	UNM C10.7	UNM 523	Skeletal-olivine-bearing	0.6
DT15	UNM C10.7	UNM 523	Porphyritic olivine-pyroxene	1
DT16	UNM C10.7	UNM 523	Porphyritic olivine-pyroxene	0.5 x 1
DT17	UNM C10.7	UNM 523	Melt-rock with relict debris	0.4 x 0.8
DT18	UNM C10.7	UNM 523	Melt-rock with relict debris	0.4 x 0.9
DT19	UNM C10.7	UNM 523	Melt-rock with relict debris	0.4
DT20	UNM C10.7	UNM 523	Melt-rock with relict debris	0.5
DT21	UNM C10.7	UNM 523	Skeletal-olivine-bearing	0.2

*USNM = United States National Museum; UNM = University of New Mexico
$^+$G-M = graphite-magnetite

INAA using standard procedures [Wakita et al., 1970; Laul and Schmitt, 1973, 1974]. Broad beam (100 μm) electron microprobe analyses of clasts and melt pockets were made to determine bulk compositions.

^{39}Ar-^{40}Ar measurements were made on a 0.201 g chip of DT4. This sample and NL-25-2 hornblende fluence monitors were irradiated with a nominal fast neutron fluence of 2 x 10^{18}. DT4 was subsequently heated for 45 minutes at each of a series of increasing temperature steps, and the isotopic composition of the extracted argon was measured on a mass spectrometer. Temperature was monitored with a thermocouple embedded in the crucible. Argon from the hornblende monitors gave ^{39}Ar/^{40}Ar ratios of 0.0312 and 0.0303, which were used to calculate ages from the Ar data for DT4. Details of the irradiation and gas extraction techniques, the hornblende monitor and the age calculations are given by Husain [1974] and Bogard et al. [1976].

Oxygen isotopic analyses of a 10.0 mg sample of clast DT3, two chips of clast DT1 (3.6 mg and 5.3 mg), and two chips of clast DT4 (4.7 mg and 2.8 mg) were carried out following previously described procedures [Clayton et al., 1976].

Results

Dimmitt consists (in vol.%) of 40±10% light-colored H4 and H5 chondritic clasts, 3±0.5% impact melt rock clasts, <0.5% shocked H chondrite clasts, 1.5±0.5% exotic clasts of non-H chondrite parentage, and 55±10% fine-grained (<2 mm) dark-colored clastic matrix (with 1% interstitial melt; A. Bischoff, personal communication, 1982), in which all clasts are embedded. No agglutinates were found.

Clasts and the clastic matrix have been shocked to the same degree: fractured silicates with undulose extinction, melt pockets and 'fizzed' troilites are common throughout the meteorite. (Shock melting of troilite produces a fine-grained fizz of irregularly-shaped grains of metallic Fe,Ni in finely crystalline troilite; Scott, 1982.) Such shock may also have caused the annealing of solar flare tracks in olivine observed by Martinek [1981]. Melt rock clast DT4 appears to have been degassed together with whole rock Dimmitt (see below). These features suggest that most of the shock occurred during or after lithification of the breccia.

Clastic Matrix

The dark-colored matrix is clastic (i.e., consists of angular mineral fragments) except for the finest-grained fraction (grain size <15 μm). This portion of the matrix was shock-melted, a process which caused lithification of the loose regolith material, forming the tough Dimmitt breccia (A. Bischoff, personal communication, 1982). The matrix contains 40 vol.% chondrules, 0.02-3.0 mm in apparent diameter, of all the textural types found in ordinary chondrites. Many of these chondrules are well defined and contain minor to abundant clear to turbid glass. Approximately 5% of the chondrules have thin rims of fine-grained opaque silicate matrix ('Huss matrix'; Huss et al., 1981) and 0.5% have rims of translucent, glassy-looking, Huss matrix [Scott et al., 1982]. Forty microchondrules (those chondrules <100 μm in diameter) of all textural types were identified [Rubin et al., 1982a]. (Dimmitt is the only regolith breccia that we have found to have a micro-

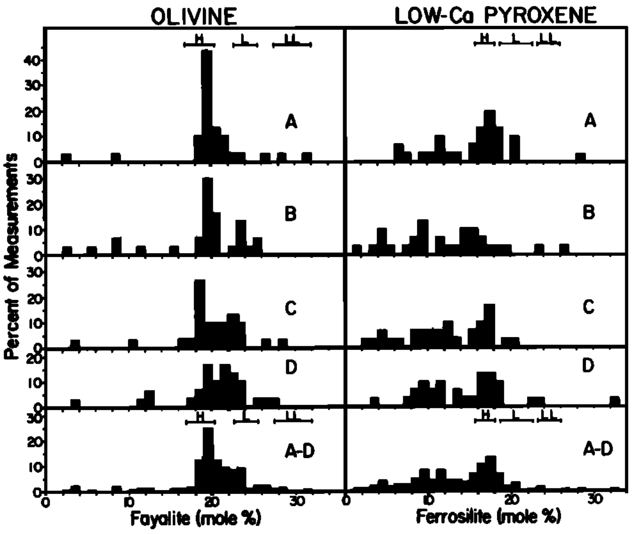

Fig. 1. Histograms of the mole% fayalite and ferrosilite concentrations in olivine and low-Ca pyroxene in different areas of the Dimmitt clastic matrix and for the entire clastic matrix. In each of the areas A-D, 30 olivines and 30 low-Ca pyroxenes were measured. The histograms indicate that different areas of the Dimmitt clastic matrix are generally similar in composition. For comparison, compositional ranges in type 4-6 ordinary chondrites are shown (revised from Gomes and Keil, 1980). Area A is from thin section UNM 523, B from UNM 547, C from USNM 1595, and D from UNM 489.

chondrule-bearing clastic matrix.) Most chondrules in the matrix are surrounded by angular mineral fragments and none appears to be part of H3 chondrite clasts.

Olivine and low-Ca pyroxene compositional patterns show peaks in the ranges characteristic of H4-6 chondrites superimposed on an unequilibrated background (Figure 1). However, low-Ca pyroxenes are more heterogeneous and more magnesian than olivines, as are those of the more equilibrated H3 chondrites (e.g., Dhajala; Noonan et al., 1976). Analyses of olivines and low-Ca pyroxenes in the matrix of four polished thin sections (areas A-D in Figure 1) indicate that low-Ca pyroxenes have very similar compositional patterns. Although olivines are broadly similar in the four areas, the proportion having compositions of Fa_{21-24} varies from 17% in area A to 40% in area D. The coefficient of variation [(σFa/mean Fa) x 100] and percent mean deviation (%MD; calculated from wt.% Fe) of 120 random olivines are 26 and 15, respectively; the corresponding numbers for 120 random low-Ca pyroxenes are 43 and 32. Olivine and low-Ca pyroxene compositional patterns of glassy chondrules in the matrix are rather similar to random matrix analyses. Olivine in the glassy chondrules shows a prominent peak at Fa_{19}, and 20% have compositions in the range Fa_{21-24}. However, the 47 analyzed glassy chondrule olivines are more heterogeneous, having a coefficient of variation of 40 and a %MD of 27.

Although the clastic matrix contains compositionally-zoned taenite with normal, M-shaped Ni profiles, taenite analyses scatter on a composition-dimension plot (Figure 2), suggesting that different grains cooled at rates of 0.2-300°C/m.y. (through 500°C). Kamacite is homogeneous with an average of 0.48 wt.% Co, typical of H4-6 chondrites [Afiattalab and Wasson, 1980].

Equilibrated Clasts

DT5 (H4) and DT6 (H5) chondrite clasts (Table 1) are petrographically indistinguishable from average H4 and H5 chondrites. DT5 contains olivine, low-Ca pyroxene (Table 2) and kamacite (0.44 wt.% Co) with compositions within the ranges characteristic of H4-6 chondrites ($Fa_{16.9-20.4}$; $Fs_{15.7-18.1}$; 0.33-0.48 wt.% Co; Gomes and Keil, 1980; Afiattalab and Wasson, 1980). Distinct chondrules and obvious chondrule fragments, 0.16-1.6 mm in apparent diameter, constitute 34 vol.% of DT5 and appear somewhat recrystallized. They do not contain glass. DT6 contains olivine, low-Ca (mostly orthorhombic) pyroxene (Table 2) and kamacite (0.45 wt.% Co), also with compositions in the ranges characteristic of H4-6 chondrites. Chondrules (0.25-3.3 mm in apparent diameter) constitute 27 vol.% of DT6. They are readily delineated, but some have extensively recrystallized boundaries and none have glass. Both DT5 and DT6 have coherent metallographic cooling rates (Figure 3) of 150°C/m.y. (using the cooling rate curves of Willis and Goldstein, 1981). Evidently, the post-lithification shock experienced by Dimmitt did not affect the central Ni contents of the taenites.

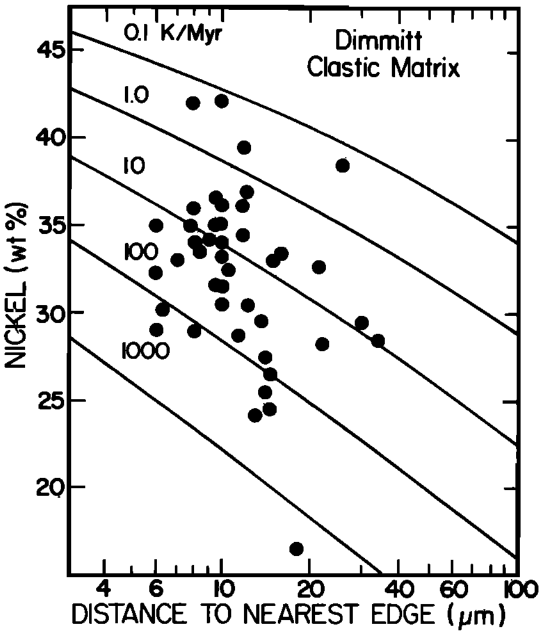

Fig. 2. Central Ni concentrations of taenite grains in the Dimmitt clastic matrix plotted against apparent distance from edge of grain. Data do not lie parallel to the cooling rate curves of Willis and Goldstein [1981] and indicate cooling rates of 0.2-300°C/m.y. at different depths before consolidation of the breccia.

Table 2. Mineralogy of Dimmitt Clasts and Clastic Matrix

Clast	Olivine	Low-Ca Pyrox	Augite	Plagioclase	k	t	Tt	FeS	Crm	Apt	Wht
Melt rock Clasts											
DT4*	M-Fa$_{20}$hm	M-Fs$_{17}$Wo$_{4}$hm	m-Fs$_{10}$Wo$_{37}$	m-Ab$_{85}$Or$_{8}$	m	m		m	a	a	a
DT9	M-Fa$_{11}$ht	M-Fs$_{13}$Wo$_{1}$ht		a-Ab$_{88}$Or$_{1}$	m				a		
DT10	M-Fa$_{21}$ht	M-Fs$_{17}$Wo$_{1}$ht		a-Ab$_{89}$Or$_{2}$	m	m	m		a		
DT11	M-Fa$_{14}$ht	M-Fs$_{5}$Wo$_{4}$ht			m		m		a		
DT12	M-Fa$_{20}$hm	M-Fs$_{17}$Wo$_{2}$hm		a-Ab$_{93}$Or$_{5}$							
DT13	M-Fa$_{11}$ht										
DT14	M-Fa$_{10}$ht										
DT15	M-Fa$_{21}$ht	m-Fs$_{20}$Wo$_{2}$ht									
DT16	m-Fa$_{23}$ht	M-Fs$_{21}$Wo$_{1}$ht	a-Fs$_{27}$Wo$_{24}$								
DT17	M-Fa$_{27}$ht										
DT18	M-Fa$_{18}$ht	M-Fs$_{17}$Wo$_{1}$hm	a-Fs$_{12}$Wo$_{24}$								
DT19	M-Fa$_{27}$ht	M-Fa$_{23}$Wo$_{2}$hm									
DT20	M-Fa$_{12}$hm	M-Fs$_{11}$Wo$_{1}$ht									
DT21	M										
Equilibrated H Chondrite Clasts											
DT5	M-Fa$_{19}$hm	M-Fs$_{16}$Wo$_{1}$ht			m	m	m	m	a	a	
DT6	M-Fa$_{19}$hm	M-Fs$_{17}$Wo$_{2}$hm	m-Fs$_{7}$Wo$_{44}$	m-Ab$_{84}$Or$_{4}$	m	m	m	m	a	a	
Shocked H Chondrite Clast											
DT7	M-Fa$_{20}$ht	M-Fs$_{20}$Wo$_{1}$ht		m-Ab$_{88}$Or$_{7}$	?	m	?	m	a		a
Exotic Clasts											
DT1^{+}	M-Fa$_{16}$ht	M-Fs$_{8}$Wo$_{1}$ht		a-Ab$_{84}$Or$_{2}$	m	m	m	M	a		a
DT2^{+}	M-Fa$_{22}$ht	M-Fs$_{17}$Wo$_{1}$ht		a-Ab$_{86}$r$_{3}$		m		m	a		a
DT3	M-Fa$_{29}$hm	M-Fs$_{24}$Wo$_{1}$hm	m-Fs$_{9}$Wo$_{44}$	m-Ab$_{86}$r$_{3}$	m	m		m	a	a	
DT8	M-Fa$_{8}$ht	M-Fs$_{10}$Wo$_{1}$ht	a-Fs$_{8}$Wo$_{25}$			m		m	a	a	a
Clastic Matrix											
Matrix	M-Fa$_{19}$ht	M-Fs$_{13}$Wo$_{1}$ht			m	m	m	m	a	a	a

M = major phase; m = minor phases; a = accesory phase; hm = homogeneous; ht= heterogeneous; k = kamacite; t = taenite; Tt = tetrataenite; Crm = chromite; Apt = chlorapatite; Wht = whitlockite.

* Also contains accessory plessite and schreibersite. +Also contains major graphite-magnetite.

Poikilitic Melt-Rock Clast

Petrography, Mineralogy, Composition and Age.

DT4, the largest melt-rock clast (Figure 4), is light in color relative to the clastic matrix. It has a prominent poikilitic texture (olivine chadacrysts enclosed by orthopyroxene oikocrysts), very similar to that of impact-melted clasts in many H, L, and LL ordinary chondrites [e.g., Keil et al., 1980; Rubin et al., 1981; Fodor and Keil, 1975]. DT4 contains olivine, low-Ca pyroxene and kamacite (0.46 wt.% Co) with compositions in the ranges characteristic of H4-6 chondrites (Table 2).

DT4 is significantly depleted in metallic Fe,Ni and troilite relative to the clastic matrix; it contains 1.1% normative metallic Fe,Ni (kamacite and taenite) and 0.05% normative troilite. Most of the metallic Fe,Ni occurs in a large (1.4 mm diameter) round assemblage of polycrystalline kamacite (crystals 8-260 μm in size, average, 38 μm; 7.0 wt.% Ni) with 5-20 μm-wide areas of plessite rimmed by taenite (24-31 wt.% Ni), and numerous 2-20 μm blebs of high-Ni schreibersite (41 wt.% Ni). Martensite and tetrataenite were not encountered.

The silicate-normalized bulk composition of clast DT4 (Table 3), determined by broad beam electron probe analysis, is very similar to that of average H chondrites [Keil, 1969], except that the clast is depleted in the volatiles Na$_2$O and P$_2$O$_5$. The rare earth element (REE) concentrations in DT4 (determined by INAA) are within one standard deviation of those of average H chondrites, except for the lighter REE, which appear to be somewhat enriched in the clast (Table 3). The Ir/Au ratio of DT4 (2.3; Table 3) is similar to that of the poikilitic melt-rock clast in the Bovedy L-group chondrite (2.1; Rubin et al., 1981) and lower than that of average H chondrites (3.7; Rambaldi et al., 1979).

DT4 has been partially degassed of its radiogenic ^{40}Ar. The ^{39}Ar/^{40}Ar ages of the temperature fractions tend to increase consistently to an age of 4.0 G.y. at an ^{39}Ar fractional release of 0.95, then to decrease abruptly (Figure 5). The K/Ca ratio remains nearly constant until the fractional ^{39}Ar exceeds 0.9, then it also decreases abruptly (Figure 5). The averaged K-Ar 'age' of DT4 is 2.70 G.y., in agreement with a Dimmitt whole rock age of 2.64 G.y.[Eberhardt et al., 1966], suggesting that DT4 was degassed together with whole rock Dimmitt.

Oxygen isotopic analysis of DT4 yields δ^{18}O and δ^{17}O values of +4.4°/oo and +3.1°/oo, respectively. The clast thus lies close to the range of whole rock values for H4-6 chondrites (Table 4, Figure 6).

Thermal history. An approximate cooling rate of DT4 can be calculated by modeling the growth of kamacite from taenite [Smith and Goldstein, 1977]. Assuming that all kamacite growth occurs at a single optimum temperature, an approximate cooling rate can be calculated by dividing the temperature interval over which kamacite growth actually occurs by the time taken to grow the average-sized kamacite grain at this temperature. Following Smith and Goldstein [1977] and Taylor et al. [1979], we find that the optimum temperature for kamacite growth in DT4 is 660°C. At that temperature, the time required to grow 38 µm-wide kamacite is 2.9x10^{11} sec, based on a diffusion coefficient that is most appropriate for the bulk composition (8.9 wt.% Ni; 0.37 wt.% P) of the assemblage [Heyward and Goldstein, 1973]. Kamacite nucleated at 710°C (corresponding to the bulk 8.9 wt.% Ni content of the assemblage) and precipitated on taenite borders as DT4 cooled. Using the Fe-Ni-P phase diagram [Romig and Goldstein, 1980], we determine that the approximate temperature at which kamacite growth ceased was 460°C [from the maximum (31 wt.%) Ni content of taenite bordering kamacite]. Thus, kamacite grew over a temperature interval of 250°C. We derive a cooling rate of 9x10^{-10} °C/sec or 30°C/10^3 y for DT4.

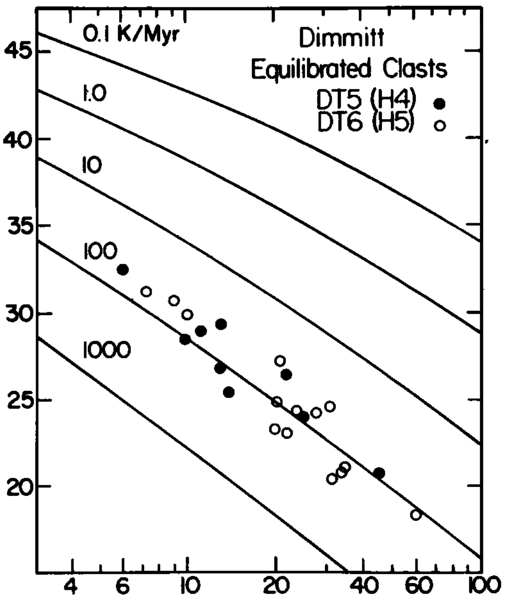

Fig. 3. Central Ni concentrations of taenite grains in equilibrated clasts DT5 (H4) and DT6 (H5) plotted against apparent distance from edge of grain. Data lie parallel to the cooling rate curves of Willis and Goldstein [1981] and indicate a cooling rate of 150°C/m.y.

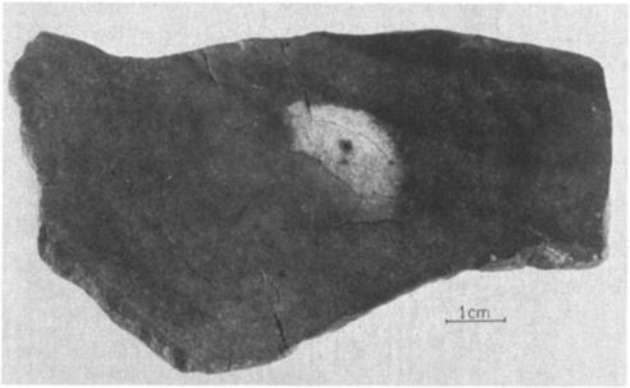

Fig. 4. Photograph of Dimmitt slab (UNM C10.9) with light-colored poikilitic melt rock clast DT4. The round metallic Fe,Ni-schreibersite assemblage in the center cooled at 30°C/10^3 y (through 500°C). The clast must have been buried beneath an 500-m-thick melt breccia pile on the floor of a several-kilometer-diameter impact crater on the H chondrite parent body.

The thermal event that formed the DT4 parent melt was an earlier more intense event than that which caused the partial loss of ^{40}Ar in DT4 discussed above. Because the melting event probably totally degassed DT4 (or its parent material) of previously accumulated ^{40}Ar, DT4 must have cooled sufficiently to retain Ar prior to 4.0 G.y. ago, which is the maximum age recorded in Figure 5.

Other Melt-Rock Clasts

The mineralogy of the other melt-rock clasts in Dimmitt is listed in Table 2. These clasts include the following:

A. Two clasts with skeletal olivine (DT14, DT21). DT14 has large elongated olivines (∿5 x 100 µm) at one end and progressively smaller olivines grading into a microcrystalline mesostasis toward the other end, which appears to be a quenched margin. Olivines in DT21 are very elongated (2 x 50 µm), but are too narrow to obtain quantitative electron probe analyses.

B. Four porphyritic clasts with olivine and

TABLE 3. Bulk Composition of Selected Clasts, H, LL, CM Chondrites and CO-CV Matrix

Element or oxide	DT4^a	DT4^b		H^c	H^d	DT8^e	CM^f	CO-CV Matrix^g	DT3^e	LL^f
SiO_2 (wt%)	49	(50.1)		48.4	(49.3)	32.5	27.3	28	44	39
TiO_2	0.09	0.16±	0.11	0.17	0.14	0.09	0.10	0.08	0.07	0.19
Al_2O_3	1.45	2.62	0.09	3.2	2.5	2.00	2.31	2.8	1.64	2.21
Cr_2O_3	0.46	0.745	0.003	0.48	0.66	0.50	0.39	0.4	0.22	0.30
FeO	15	14.9	0.3	11.8	12.7	33.9	25.5	32	23	27
MgO	31	27.9	0.7	31.1	31.0	21.3	19.0	19	28	25
MnO	0.46	0.369	0.001	0.33	0.38	0.36	0.17	0.2	0.38	0.32
CaO	2.58	2.0	0.2	2.41	2.2	0.80	2.03	1.5	1.25	1.96
Na_2O	0.64	1.051	0.008	1.13	1.01	0.21	0.54	0.34	0.66	0.87
K_2O	0.11	0.16	0.07	0.19	0.13	0.07	0.05	0.04	0.13	0.21
P_2O_5		0.04			0.30		0.35	0.27	0.06	0.22
H_2O				0.44			13.2			0.37
NiO						1.31	1.76	1.2	0.41	1.21
S						1.13	3.1	0.5	0.72	2.14
C						1.	2.44			
Sc (ppm)		10.7	0.1		9.9					
V		88	4		80					
Co		69	1		834					
Ni		600	25		16900					
La		0.75	0.07		0.42					
Sm		0.31	0.01		0.26					
Eu		0.10	0.03		0.101					
Dy		0.06	0.05		0.43					
Yb		0.27	0.09		0.26					
Lu		0.05	0.02		0.046					
Hf		0.3	0.1		0.24					
Au (ppb)		7	2		210					
Ir		16	3		730					
Total (wt%)	100.8	100		99.95	100	95.52	98.16	86.1	100.5	101.

All Fe as FeO and all Ni as NiO.

[a] Silicate-normalized bulk composition (determined by broad-beam electron probe analysis).

[b] Average of two analyses, INAA, (SiO_2 by difference).

[c] Silicate-normalized bulk composition [after Keil, 1969].

[d] Averages compiled from Evensen et al. [1978]; Felsche and Hermann [1970]; Mason [1965, 1971, 1979]; Masuda et al, [1973]; Nakamura [1974]; Schmitt et al. [1972]; and Shima [1979]. The values for Co, Ni, Au and Ir are for bulk H chondrites; all other values are for silicate portions of H chondrites (INAA; SiO_2 by difference).

[e] Bulk compositions (determined by broad-beam electron probe analysis).

[f] Bulk composition [after Keil, 1969].

[g] Bulk composition [McSween and Richardson, 1977].

low-Ca pyroxene phenocrysts (DT12, DT13, DT15, DT16). These clasts appear somewhat similar to large porphyritic chondrules, but differ from them primarily in having nonspherical shapes.

C. Seven clasts which contain relict, apparently unmelted silicate grains with partially resorbed margins and heterogeneous compositions (Table 2) set in a dark-colored microcrystalline groundmass (DT9, DT10, DT11, DT17, DT18, DT19, DT20). In addition, numerous smaller such clasts, 0.05-0.2 mm in maximum dimension, were also observed. These debris-laden clasts are the most abundant type of melt rock clast in Dimmitt, constituting half of all of the melt rock clasts large enough for microscopic examination. DT11 contains a 200 µm-diameter relict porphyritic pyroxene chondrule (Fs_6Wo_3) with partially resorbed margins. It also contains an isotropic glass shard (0.1 mm in maximum dimension) similar in composition to the glassy mesostases of some chondrules from type 3 ordinary chondrites [Gooding, 1979]; the shard thus may have been derived from a fragmented chondrule. Clasts similar to these seven occur in Plainview (e.g., PV5b and PV7b of Fodor and Keil, 1976), in the Adams County H5 chondrite [Fodor et al., 1980] and in the Vishnupur LL6 chondrite [Fodor and Keil, 1978]. They formed in the regolith by impact-melting accompanied by loss of metallic Fe,Ni and sulfide as an immiscible liquid and incorporation of unmelted regolith materials before quenching.

Shocked H Chondrite Clast

DT7 is an angular clast containing a very fine-grained, opaque matrix (∿ 85 vol.%) consisting of silicates with finely dispersed, very abundant, small (<1 µm) grains of metallic Fe,Ni and troilite. Subhedral to anhedral olivine,

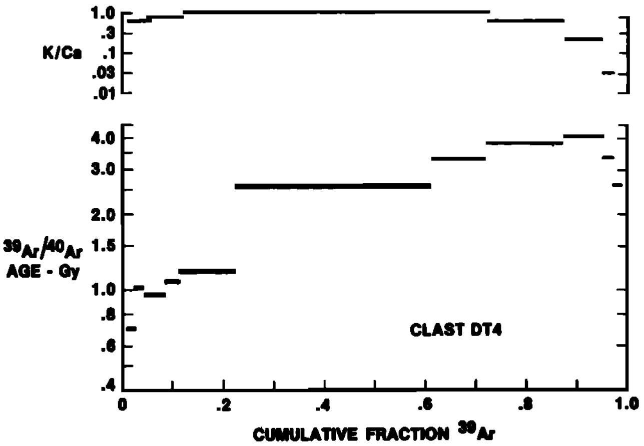

Fig. 5. Calculated ^{39}Ar/^{40}Ar ages and K/Ca ratios of clast DT4 as a function of fraction of ^{39}Ar released, from stepwise temperature extractions.

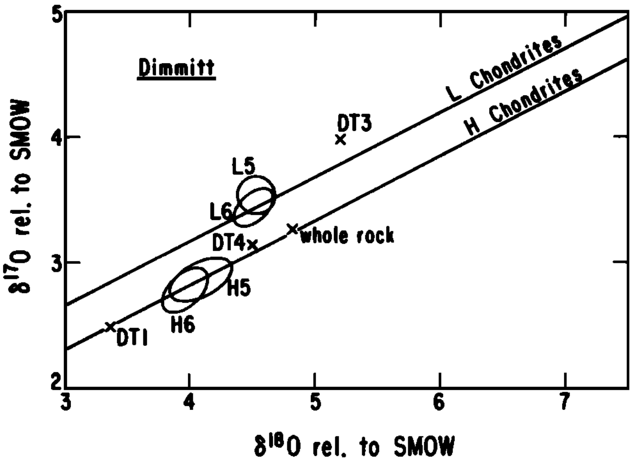

Fig. 6. Three isotope plot showing Dimmitt whole rock and clasts DT1 (a type 3 chondrite with a graphite-magnetite matrix), DT3 (LL5 chondrite) and DT4 (poikilitic melt rock of H chondrite composition) compared to the 1 ranges for types 5-6 H and L chondrites. Dimmitt whole rock lies beyond the range of H5-6 chondrites; this may be due to terrestrial weathering or to the presence in Dimmitt of somewhat ^{18}O-enriched type 3 material.

low-Ca pyroxene, and plagioclase grains (Table 2), 2-40 µm in maximum dimension, constitute 15 vol.% of the clast. The dispersion of the metallic Fe,Ni and sulfide grains suggests that these phases were mobilized by shock. Olivine is heterogeneous, but has an average composition within the range of H4-6 chondrites, although low-Ca pyroxene (also heterogeneous) has an average composition in the range characteristic of L4-6 chondrites (Table 2). Bulk atomic ratios of Ca/Si, Fe/Si and Mg/Si are in the ranges characteristic of ordinary chondrites [Wasson, 1974]. The texture of DT7 as well as its mineral and bulk compositions indicate that this clast was probably derived from the heterogeneous Dimmitt clastic matrix by shock.

Clasts of Different Chondrite Groups

Four chondritic clasts, not of H-group classification, were discovered; such clasts constitute 1% of the Dimmitt breccia. These include an LL5 clast (DT3), two clasts of a new kind of type 3 chondrite with a graphite-magnetite matrix (DT1, DT2), and a carbonaceous chondrite clast (DT8).

LL5 Chondrite Clast. The bulk chemical composition (determined by broad beam electron probe analysis), olivine, low-Ca pyroxene and kamacite compositions, and modal abundance of metallic Fe,Ni all indicate that clast DT3 is an LL-group chondrite (Tables 3 and 4). However, its total Fe content and oxygen isotopic composition are slightly outside the LL ranges, but in both cases, they are even farther from the H and L chondrite ranges (Table 5; Figure 6). (The LL range is not shown in Figure 6 because only three LL5-6 chondrites have been measured.) DT3 contains barred olivine, porphyritic olivine and cryptocrystalline chondrules (0.4-2.0 mm in diameter) with recrystallized boundaries, set in a recrystallized silicate matrix. The recrystallized nature of the chondrules and silicate matrix, presence of augite, fairly homogeneous compositions of olivine (%MD=2) and low-Ca pyroxene (%MD=5), and abundance of small (3-5 µm) grains of plagioclase composition and stoichiometry (Table 2) indicate that the clast is of petrologic type 5. Shock veins, melt pockets, and undulose extinction and extensive

TABLE 4. Properties of DT3 (LL5 Clast) in Dimmitt Compared to Ordinary Chondrites

Parameter	LL5 Clast	LL	L	H
Olivine (mole % Fa)[*]	29.0	27.5 -32	22.7 -25.6	16.9 -20.4
Low-Ca Pyroxene (mole % Fs)[*]	24.3	23.2 -26	18.7 -22.6	15.7 -18.1
Kamacite (wt. % Co)[+]	2.8	1.5 -11.0	0.67-0.82	0.33-0.48
Metallic Fe,Ni (wt.%)[*]	3.1	3.0 -6.0	4.4 -11.7	14.2 -19.8
Bulk Fe/Si (atomic)[¢]	0.44	0.38-0.58	0.50-0.65	0.67-0.93
Total Fe (wt.%)[*]	18.0	18.9 -22.5	20.5 -23.3	25.3 -30.9

[*] Type 4-6 ordinary chondrites, including Parambu [Gomes and Keil, 1980].
[+] Affiattalab and Wasson [1980].
[¢] Wasson [1974] with data for Parambu [Gomes and Keil, 1980].

TABLE 5. Oxygen Isotopic Compositions of Dimmitt Clasts

Sample	$^{18}O\ ^{o}/oo$	$^{17}O^{o}/oo$	Δ^{17*}
Whole rock	4.8	3.3	0.8
DT1	3.4	2.5	0.8
DT3	5.2	4.0	1.3
DT4	4.4	3.1	0.8
H4-6	3.8-4.7	2.7-3.2	0.8
L4-6	4.4-4.7	3.4-3.7	1.1
LL4-6	4.7-5.0	3.5-3.8	1.1

* Δ^{17} is the apparent ^{17}O excess relative to the terrestrial fractionation line. $\Delta^{17}=\delta^{17}-0.516\delta^{18}$ For 24 H chondrites, $\Delta^{17}= 0.77 \pm 0.04$; for 17 L chondrites, $\Delta^{17}= 1.12 \pm 0.04$; for 6 LL chondrites, $\Delta^{17}= 1.13 \pm 0.11$.

fracturing of silicates indicate that the clast is of shock facies d [Dodd and Jarosewich, 1979]. We thus classify the clast as an LL5d chondrite.

Chondrites Rich in Graphite-Magnetite. Clasts DT1 and DT2 are of a new kind of type 3 chondrite with a graphite-magnetite matrix [Scott et al., 1981a,b]. They contain heterogeneous olivines and low-Ca pyroxenes (Table 2), olivines with 0.1 wt.% CaO, well-defined glassy chondrules (100-500 μm in apparent diameter), and bulk Al/Si, Mg/Si, Ca/Si, and Fe/Si atomic ratios in or very near the ordinary chondrite range. Two other clasts of this new kind of type 3 chondrite were found in the Plainview and Weston H chondrite regolith breccias [Scott et al., 1981a,b]. The matrix of these clasts is composed of fine-grained graphite and magnetite, rather than the fine-grained opaque and recrystallized silicate matrix ['Huss matrix'; Huss et al., 1981] normally found in type 3 ordinary chondrites. Most of the graphite-magnetite has very little metallic Fe,Ni embedded in it.

Oxygen isotopic analysis of DT1 gave $\delta^{18}O = +3.4^{o}/oo$, $\delta^{17}O = +2.5^{o}/oo$ (Table 5; Figure 6). This point lies on a mass-fractionation line through the data for H4-6 chondrites, but is displaced toward lower $\delta^{18}O$ and $\delta^{17}O$ values by 0.7 and $0.4^{o}/oo$, respectively, from the H4-6 chondrite region. This displacement may be a result of light isotope enrichment in magnetite relative to olivine and pyroxene [Anderson et al., 1971].

Carbonaceous Chondrite Clast. DT8 is an angular clast that contains 80 vol.% fine-grained, predominantly opaque silicate matrix, 5 vol.% of 25 μm taenites and 10 μm troilites, and 15 vol.% subhedral to anhedral olivine and pyroxene grains (1-140μm). Some rounded aggregates of olivine and pyroxene may be porphyritic chondrule fragments. The abundance of large silicate grains distinguishes DT8 from clasts of fine-grained opaque silicate matrix which are present in some type 3 ordinary chondrites.

Analyses of 14 olivines (Fa_{3-12}; avg. Fa_{8}; $\sigma_{Fa} = 3$) and 10 low-Ca pyroxenes (Fs_{0-38}; avg. Fs_{10}; $\sigma_{Fs} = 12$) indicate that these minerals are more magnesian than those of ordinary chondrites and are similar to those of some carbonaceous chondrites, particularly the CV group [McSween, 1977]. However, in this clast, low-Ca pyroxenes are on average slightly more Fe-rich than olivines, unlike most CV chondrites [McSween, 1977]. The bulk composition of DT8 is more Fe-rich than bulk CO-CV chondrites [Keil, 1969], but is more similar to that of CO-CV opaque matrix (Table 3). DT8 has a high modal matrix abundance, like CM chondrites [McSween, 1979], but is higher in FeO and SiO_2 and lower in CaO and S than average CM chondrites. From the high total of the bulk analysis, it is apparent that DT8 is lower in H_2O and C relative to CM chondrites, but not CO-CV matrix (Table 3). We conclude that DT8 is a fragment of some kind of carbonaceous chondrite, probably of petrologic type 3. However, the present data are insufficient to render a more specific identification.

Graphite-Magnetite Aggregates

Numerous 30 μm to 1 mm clasts of graphite-magnetite aggregates make up 1 wt.% of Dimmitt [Scott et al., 1981a]. These aggregates are very similar in texture and composition to the graphite-magnetite matrix areas of DT1 and DT2. Such aggregates were probably derived from fragmented clasts of chondrites like DT1 and DT2 [Scott et al., 1981a]. Isolated graphite-magnetite aggregates have been identified within the clastic matrices of other H and L chondrite regolith breccias as well as in several type 3 ordinary chondrites [Scott et al., 1981a; McKinley et al., 1981]. The graphite-magnetite aggregates in type 3 ordinary chondrites generally contain more metallic Fe,Ni than the graphite-magnetite aggregates in the regolith breccias.

Discussion

Nature of Clastic Matrix

Low-Ca pyroxenes in the Dimmitt clastic matrix are very heterogeneous (Figure 1) but do exhibit a peak in their compositional distribution in the range characteristic of H4-6 chondrites ($Fs_{15.7-18.1}$; Gomes and Keil, 1980). The olivine compositional distribution is more complicated and comprises three components: a prominent peak in the range characteristic of H4-6 chondrites ($Fa_{16.9-20.4}$; Gomes and Keil, 1980), constituting 40% of the analyses, a minor peak at Fa_{21-24}, constituting 20%, and a background of unequilibrated olivines, ranging from Fa_{2-32}. These three components constitute somewhat different proportions in the four analyzed areas (A-D). For example, the minor Fa_{21-24} peak is most prominent in areas C and D (where it constitutes 30% of the olivines) and least prominent in area A (where it constitutes 7%). Compositional distribution histograms of olivines in the matrices of most H chondrite regolith breccias [e.g., Noonan and Nelen, 1976; Keil and Fodor, 1980; McSween and Lipschutz, 1980; McSween et al., 1981] are similar to that of the Dimmitt matrix in having prominent peaks in the range characteristic of H4-6 chondrites superimposed on an unequilibrated background. The proportion of olivines in the H4-6 range in the Dimmitt matrix (40±5%) is comparable to that of Tysnes Island (50±5%), Weston (50±5%), and parts of Leighton (20±5% in FD3) [McSween and Lipschutz, 1980; McSween et al., 1981]. [In some regolith breccias, e.g., Pantar II (but not Pantar I), (Fredriksson and Keil, 1963; Lipschutz et al., 1982) and, to lesser extents, Nulles and Cangas de Onis (A. E. Rubin, unpublished data), matrix olivines are almost completely equilibrated.] However, the minor olivine peak at Fa_{21-24}, which we found in the Dimmitt matrix, has not been observed in other H chondrite regolith breccias. The area-to-area matrix heterogeneity in Dimmitt seems to be smaller than that in Leighton [McSween et al., 1981] and Pantar [Lipschutz et al., 1982].

The simplest explanation for these olivine and low-Ca pyroxene compositional distributions is that they result from the non-uniform admixture of unequilibrated material to comminuted equilibrated clasts [e.g., McSween and Lipschutz, 1980]. About 20% of the glassy chondrules in the Dimmitt matrix (which must be part of the unequilibrated component) also have olivine compositions in the range of H4-6 chondrites, Fa_{17-20}. This indicates that the prominent peak in this compositional range in the Dimmitt matrix is not due entirely to olivines broken out of equilibrated clasts.

It is unlikely that the unequilibrated component in the breccia matrices is primarily normal H3 material. The least equilibrated ordinary chondrites (petrologic types 3.0-3.5; Sears et al., 1980), which have the most heterogeneous olivines, contain 10-15 vol.% fine-grained opaque silicate matrix [Huss, 1979]. This material is relatively rare in H chondrite regolith breccias; we have only found it as thin rims around 5% of the chondrules in the Dimmitt matrix and around 1% of the chondrules in the matrix of Cangas de Onis. In addition, H3 clasts are very rare in H chondrite regolith breccias; they have been reported only in Weston [Noonan and Nelen, 1976]. Evidently, H3 clasts were far less abundant in the H chondrite parent body regolith than were carbonaceous chondrite clasts. Thus normal consolidated H3 material is probably not a major source of the unequilibrated component in the Dimmitt matrix.

Nevertheless, the occurrence of opaque matrix rims around 5% of the chondrules in the Dimmitt matrix suggests that the matrix contains a minor H3.0-3.5 component. [This same component may have contributed the microchondrules to Dimmitt, because Rubin et al. (1982a) determined that, among type 3 chondrites, microchondrules are most abundant in the H and CO groups.] The approximate volume of opaque matrix material in the Dimmitt matrix (0.2±0.2%) was derived from the proportion of chondrules that have opaque matrix rims (5%), the abundance of chondrules in the matrix (40%), and the maximum (opaque matrix rim volume)/(chondrule volume) ratio (10%). Because type 3.0-3.5 ordinary chondrites contain 10-15 vol.% opaque matrix [Huss, 1979] and the Dimmitt clastic matrix contains 0.2 vol.% opaque matrix, then 2 vol.% of the matrix consists of normal H3.0-3.5 material.

The graphite-magnetite aggregates in the clastic matrices of ordinary chondrite regolith breccias were probably derived from fragmented graphite-magnetite-rich type 3 chondrites like DT1 and DT2 [Scott et al., 1981a]. Chondrules and silicate grains from such chondritic clasts must also contribute to the unequilibrated component of the clastic matrices. The glassy chondrules in the Dimmitt matrix are smaller than those of most H3 chondrites: 75±5% of them are 500 µm in apparent diameter. These chondrules are similar in size to those in the graphite-magnetite-rich chondrites (100-500 µm; Scott et al., 1981b), but are also of similar size to glassy chondrules in the Willaroy H3 chondrite (A. E. Rubin, unpublished data). Olivine and low-Ca pyroxene histograms very similar to those of the Dimmitt clastic matrix (including a minor olivine peak at Fa_{21-24}) can be obtained by combining the histograms of DT1 and DT2 [Scott et al., 1981b], and assuming both clasts contribute equally to the Dimmitt matrix. However, DT2 is small (1 mm) and contains only about 5 chondrules; thus its olivine and low-Ca pyroxene histograms may not be representative. The Dimmitt matrix contains roughly 2 vol.% graphite-magnetite aggregates. Clast DT1 contains 15 vol.% graphite-magnetite [Scott et al., 1981b]; hence, 10-15% of the clastic matrix is probably derived from graphite-magnetite-rich chondrite clasts.

Some small proportion of the Dimmitt matrix may come from H3.6-4.0 chondrites. These contain 1-4 vol.% opaque silicate matrix material and 30% of their olivines have compositions outside the H4-6 range of Fa_{17-20} [Dodd et al., 1967; Noonan et al., 1976]. However, the published compositional distributions of olivines in H3.6-4.0 chondrites do not show a minor peak at Fa_{21-24}, as does the Dimmitt matrix. The source of these olivines is unknown.

Thus the unequilibrated material in the Dimmitt matrix probably consists of at least three components: 10 - 15% from graphite-magnetite-rich chondrites, 2% normal H3.0-3.5 material, and the remainder from another source. This third (unidentified) source contains relatively small chondrules (most of which are 500 µm in diameter), olivines with a minor compositional distribution peak at Fa_{21-24}, but very little fine-grained opaque silicate matrix. Because most of the chondrules in the Dimmitt matrix are surrounded by mineral grains and fragments and do not appear to be attached to other components in the regolith, most of the chondrules in the third unequilibrated component were probably added to the Dimmitt regolith as isolated or only loosely-consolidated objects.

Origin of Exotic Clasts

Dimmitt's exotic materials include a carbonaceous chondrite clast and the best documented example of a clast of an ordinary chondrite (LL5) residing in a host of a different ordinary chondrite chemical group (H). Other similar, but less well-described examples, are two H5±1 chondrite clasts in the St. Mesmin LL chondrite regolith breccia [Dodd, 1974] and an LL4±1 clast in the unique Bencubbin breccia [Kallemeyn et al., 1978]. Because graphite-magnetite aggregates have been found in predominantly unbrecciated H3 chondrites (e.g., Sharps;

Scott et al., 1981a), it is not clear that these aggregates or the graphite-magnetite-rich chondrite clasts (DT1 and DT2) should be considered exotic.

Most workers [e.g., Wilkening, 1977; Wasson and Wetherill, 1979] consider exotic clasts to be meteoroid projectiles that impacted their meteorite hosts' parent bodies late in solar system history (4 G.y. ago) at sufficiently low relative velocities to avoid vaporization or complete melting. We agree that some exotic clasts (e.g. carbonaceous chondrite clasts in the Kapoeta howardite; Wilkening, 1973) were incorporated in just this manner. However, Fodor et al. [1976] suggested that some non-H chondrite rock types may have accreted along with H chondrite material to form the H chondrite parent body early in solar system history (4.5 G.y. ago). The occurrence of carbonaceous chondrite clasts in the Mezö-Madaras L chondrite that experienced mild post-accretion metamorphism [Van Schmus, 1967] is consistent with this suggestion.

In the metamorphosed-planetesimal model of Scott and Rajan [1981], maximum metamorphic temperatures (from an ^{26}Al heat source) occurred on planetesimals about 20 km in diameter that subsequently accreted into larger objects before their residual heat was lost. Because exotic clasts constitute 1.5±0.5 vol.% of Dimmitt, it is possible that 1-2% of the planetesimals that accreted to form the H chondrite parent body were of non-H chondrite parentage. These materials could have formed widely-separated 'exotic outcrops' on the surface of the H chondrite parent body. Impacts into the exotic outcrops would have dispersed exotic clasts into the H chondrite parent body regolith. Because Abbott and Plainview contain more carbonaceous chondrite clasts than Dimmitt, and Dimmitt contains more graphite-magnetite aggregates (assuming that they are exotic) than Abbott and Plainview, it is apparent that each H chondrite regolith breccia has its own unique complement of exotic clasts. These differences could reflect breccia consolidation at different times, after sporadic impacts into exotic outcrops dispersed certain exotic clasts throughout the entire parent body regolith. Alternatively, differences in exotic clast abundances in breccias could reflect spatial regolith heterogeneities.

We can estimate whether such exotic planetesimals would have retained their characteristic oxygen isotopic compositions during thermal metamorphism. Using the diffusion data of Giletti et al. [1978], we calculate that oxygen will diffuse a maximum of 10-15 m in feldspar upon cooling from a maximum temperature of 900°C [Onuma et al., 1972] to 400°C at very slow cooling rates (1°C/m.y.). More rapid cooling results in smaller diffusion distances. Oxygen self-diffusion in forsterite [Jaoul et al., 1980] is much slower than for feldspars. Additional evidence for slow diffusion of oxygen comes from Olsen et al. [1981], who showed that anomalous oxygen diffused over a distance of only a few millimeters in a cristobalite-pyroxene assemblage (CRISPY) in an L6 chondrite. Thus if exotic (i.e., non-H chondritic) planetesimals >1 km in size had accreted hot to the H chondrite parent body early in solar system history, the amount of oxygen isotopic equilibration with H material would have been trivial. Hence the occurrence of exotic clasts in chondrite regolith breccias (e.g., the LL clast in Dimmitt) with oxygen isotopic compositions different from that of the hosts (Table 4; Figure 6) is as equally consistent with the clasts' derivation from exotic outcrops as from late-accreted projectiles.

Complexity of Parent Body Surface Processes

The cooling rate of DT4 (the large poikilitic clast) of 30°C/10^3 y can be used to estimate its burial depth [Taylor et al., 1979; Rubin et al., 1981]. If an extremely low thermal diffusivity (10^{-4} cm^2/sec), comparable to that of the lunar regolith [Langseth et al., 1976], is assumed for the material overlying DT4, then a burial depth of 100 m is indicated; if a higher thermal diffusivity (10^{-2} cm^2/sec), typical of chondritic material [Wood, 1967], is assumed, then a burial depth of 1000 m is indicated. We thus estimate that DT4 was buried at a depth on the order of 500 m when it cooled through 500°C.

From this cooling rate and burial depth, we infer a complex history for DT4: (a) impact melting of material at or near the surface of the H chondrite parent body to form the clast and immediate burial to depths of 500 m, (b) cooling of the clast through 500°C at 30°C/10^{3}y, (c) impact excavation and incorporation of the clast into the regolith, and (d) consolidation of this portion of the regolith to form the Dimmitt breccia, accompanied by partial degassing of radiogenic ^{40}Ar with subsequent removal of the breccia from the H chondrite parent body by collision. Such complexity is probably characteristic of asteroidal regolith processes.

In order for the poikilitic melt rock, represented by DT4, to have avoided quenching, it must have been buried beneath hot material almost immediately after it formed. This probably constrains the formation location to be on the bottom of an 500-m-thick melt breccia pile on the floor of an impact crater that was several kilometers in diameter. Terrestrial impact craters have similarly thick melt breccia piles (e.g., 600 m in the 3.8-km-diameter Brent Crater in Canada; Dence, 1968). In order for DT4 to have been excavated from this depth, another high-energy impact (or a series of lower-energy impacts) must have occurred at the same locality, causing the removal of >500 m of overlying material.

Comparison to Accretionary and Lunar Regolith Breccias

Despite the antiquity of nearly all of the components in chondrite regolith breccias [Wetherill, 1982], these breccias could not have formed during accretion of the H chondrite parent body. All ten H chondrite regolith breccias that have been analyzed contain equilibrated H chondrite clasts that have coherent metallographic cooling rates between 10 and 150°C/m.y. [Scott and Rajan, 1981; Figure 3; A. E. Rubin, unpublished data], in the same range as those of individual equilibrated ordinary chondrites [e.g., Wood, 1967; Taylor and Heymann, 1971; Scott and Rajan, 1981]. These slow cooling rates require burial depths of tens of kilometers [e.g., Wood, 1967], implying the existence of a large parent body prior to the consolidation of the regolith breccias. In addition, the occurrence of a 3.6 G.y. old impact melt rock clast in Plainview [Keil et al., 1980] indicates that consolidation of one of these breccias took place at least 10^9 y after accretion.

Chondrite regolith breccias are much coarser-grained than their lunar counterparts; 96 wt.% of the grains in 72441,7 (a typical South Massif lunar soil) are < 2 mm in size [Heiken, 1975], whereas only 55±10 vol.% of the constituents of Dimmitt (i.e., the clastic matrix) are <2 mm. Other differences between meteorite and lunar regolith breccias include the much lower abundance in meteorite breccias of impact glass, agglutinates, glass spheres, micrometeorite craters on glass spheres, solar-wind-implanted ^{4}He, and mineral grains rich in solar flare particle tracks [e.g., Housen et al., 1979]. Although exotic clasts (i.e., meteorite fragments) are very rare on the moon, approximately 1.9% of the lunar regolith consists of admixed carbonaceous chondrite material, recognizable by its geochemical signature [Ganapathy et al., 1970]. This is comparable to the 1.5±0.5 vol.% exotic clasts in Dimmitt, although the Dimmitt matrix may contain additional pulverized exotic materials.

Conclusion

By analogy with lunar regolith breccias, which contain the same constituents as unconsolidated lunar regolith, meteorite regolith breccias are probably representative samples of meteorite parent body regoliths. Dimmitt, and therefore the regolith from which it formed, contains (in vol.%) 40±10% centimeter-sized, slowly-cooled, equilibrated H4 and H5 clasts, 3±0.5% impact melt rock clasts (<0.2-24 mm in size), ≤0.5% shock-blackened H chondrite clasts (≤1 mm in size), 1.5±0.5% exotic clasts of non-H chondrite parentage (including a 3 mm carbonaceous chondrite and a 14 mm LL5 chondrite), and 55±10% fine-grained (<2 mm), dark-colored, clastic matrix (with 1% interstitial melt), in which the clasts are embedded. No agglutinates were found; documented agglutinates from H chondrite regolith breccias are known only from Fayetteville [e.g., Kerridge and Kieffer, 1977; Taylor 1982] and, apparently, were rare in the regolith. No normal H3 chondrite clasts were found; such clasts were also rare in the regolith and are known only from Weston [Noonan and Nelen, 1976]. Although chondrite regoliths differ from the lunar regolith in a number of respects, including having a much coarser grain size, both regoliths contain a few percent exotic materials. In lunar soils, the exotic materials are generally pulverized and are recognized geochemically; in chondrite regoliths, exotic materials occur as discrete clasts (although additional pulverized exotic material may be present).

The clastic matrices of H chondrite regolith breccias consist of comminuted, equilibrated H chondrite clasts and unequilibrated material. The unequilibrated material in Dimmitt's matrix contains glassy chondrules (most < 500 μm in diameter), olivines that have a minor compositional distribution peak at Fa_{21-24}, and little fine-grained, opaque silicate matrix. This unequilibrated material contains 10-15% material from graphite-magnetite-rich chondrites and 2% H3.0-3.5 chondrite material. Some of the remainder may consist of H3.6-4.0 material, but the source of the minor olivine peak at Fa_{21-24} is unknown. Although abundant, the unequilibrated material does not occur as clasts, and hence may exist on the H chondrite parent body primarily as unconsolidated material.

Exotic clasts in chondrite regolith breccias are either late accreted projectiles or were derived from exotic outcrops on the parent body surface. These outcrops could be fragments of exotic planetesimals that accreted to the H chondrite parent body early (4.5 G.y. ago) in solar system history. Even if temperatures were on the order of 900°C when the planetesimals accreted, diffusion would not have altered the exotic planetesimals' original oxygen isotopic compositions. If impacts into exotic outcrops disperse exotic clasts throughout the entire parent body regolith, then regolith breccias (each with its own unique abundance of various kinds of exotic clasts) were consolidated from the regolith at different times.

Some slowly-cooled impact melt rock clasts (e.g., DT4 in Dimmitt) were probably formed beneath deep (hundreds of meters) melt breccia piles on the floors of impact craters that were several kilometers in diameter. Subsequent impacts at the same locality were necessary to excavate such clasts and deposit them in the regolith. Such complexity is probably characteristic of asteroidal regolith processes.

The occurrence in H chondrite regolith breccia clastic matrices of compositionally-zoned taenite grains that appear to have cooled at different rates (e.g., Figure 2) at different depths [Scott and Rajan, 1981], has been interpreted as indicating that ordinary chondrite parent bodies were disrupted by very high-energy impacts and then reassembled gravitationally [Rubin et al., 1982b; Taylor et al., 1982]. Many large asteroids [Davis and Chapman, 1977; Davis et al., 1979; Hartmann, 1979] and eight of Saturn's satellites [Smith et al., 1982] probably experienced such episodes of disruption and reassembly.

Acknowledgments. We thank M.-S. Ma and R. A. Schmitt (Oregon State University) for their unpublished instrumental neutron activation analysis of clast DT4, E. J. Olsen (Field Museum of Natural History) for supplying a sample of Dimmitt whole rock for oxygen isotope analysis, A. Bischoff for discussions, and G. H. Conrad for technical assistance. This work was supported in part by National Aeronautics and Space Administration grant NGL 32-004-064 (K.K.) and National Science Foundation grant EAR-78-23680 (R.N.C.).

References

Afiattalab, F., and J. T. Wasson, Composition of the metal phases in ordinary chondrites: implications regarding classification and metamorphism, Geochim. Cosmochim. Acta, 44, 431-446, 1980.

Anderson, A. T., R. N. Clayton, and T. K. Mayeda, Oxygen isotope thermometry of mafic igneous rocks, J. Geol., 79, 715-729, 1971.

Bogard, D. D., L. Husain, and R. J. Wright, ^{40}Ar-^{39}Ar dating of collisional events in chondrite parent bodies, J. Geophys. Res., 81, 5664-5678, 1976.

Clayton, R. N., N. Onuma, and T. K. Mayeda, A classification of meteorites based on oxygen isotopes, Earth Planet. Sci. Lett., 30, 10-18, 1976.

Davis, D. R. and C. R. Chapman, The collisional evolution of asteroid compositional classes (abstract), in Lunar Science VIII, pp. 224-226, The Lunar Science Institute, Houston. 1977.

Davis, D. R., C. R. Chapman, R. Greenberg, S. J. Weidenschilling, and A. W. Harris, Collisional evolution of asteroids: populations, rotations, and velocities, in Asteroids, edited by T. Gehrels, pp. 528-557, Univ. Arizona, Tucson, 1979.

Dence, M. R., Shock zoning at Canadian Craters: petrography and structural implications, in Shock Metamorphism of Natural Materials, edited by B. M. French and N. M. Short, pp. 169-184, Mono, Baltimore 1968.

Dodd, R. T., Petrology of the St. Mesmin chondrite, Contrib. Mineral. Petrol., 46, 129-145, 1974.

Dodd, R. T., and E. Jarosewich, Incipient melting in and shock classification of L-group chondrites, Earth Planet. Sci. Lett., 44, 335-340, 1979.

Dodd, R. T., W. R. Van Schmus, and D. M. Koffman, A survey of the unequilibrated ordinary chondrites, Geochim. Cosmochim. Acta, 31, 921-951, 1967.

Eberhardt, P., O. Eugster, J. Geiss, and K. Marti, Rare gas measurements in 30 stone meteorites, Z. Naturforsch., 21a, 414-426, 1966.

Evensen, N. M., P. J. Hamilton, and R. K. O'Nions, Rare-earth abundances in chondritic meteorites, Geochim. Cosmochim. Acta, 42, 1199-1212, 1978.

Felsche, J., and A. G. Hermann, Yttrium and lanthanides, in Handbook of Geochemistry, edited by K. H. Wedepohl, vol. II-5, Springer, Heidelberg, 1970.

Fodor, R. V., and K. Keil, Composition and origin of lithic fragments in L- and H-group chondrites (abstract), Meteoritics, 8, 366-367, 1973.

Fodor, R. V., and K. Keil, Implications of poikilitic textures in LL-group chondrites, Meteoritics, 10, 325-339, 1975.

Fodor, R. V., and K. Keil, Carbonaceous and non-carbonaceous lithic fragments in the Plainview, Texas chondrite: origin and history, Geochim. Cosmochim. Acta, 40, 177-189. 1976.

Fodor, R. V., and K. Keil, Catalog of lithic fragments in LL-group chondrites. UNM Inst. Meteoritics Spec. Pub., 19, Univ. New Mexico, Albuquerque, 1978.

Fodor, R. V., K. Keil, L. L. Wilkening, D. D. Bogard, and E. K. Gibson, Origin and history of a meteorite parent-body regolith breccia: carbonaceous and non-carbonaceous lithic fragments in the Abbott, New Mexico chondrite, in Tectonics and Mineral Resources of Southwestern North America, New Mexico Geol. Soc. Spec. Pub., 6, 206-218, 1976.

Fodor, R. V., K. Keil, M. Prinz, M.-S. Ma, A. V. Murali, and R. A. Schmitt, Clast-laden melt-rock fragment in the Adams County, Colorado H5 chondrite, Meteoritics, 15, 41-62, 1980.

Fredriksson, K., and K. Keil, The light-dark structure in the Pantar and Kapoeta stone meteorites, Geochim. Cosmochim. Acta, 27, 717-739, 1963.

Ganapathy, R., R. R. Keays, J. C. Laul, and E. Anders, Trace elements in Apollo 11 lunar rocks: implications for meteorite influx and origin of moon, Proc. Apollo 11 Lunar Sci. Conf., 1117-1142, 1970.

Giletti, B. J., M. P. Semet, and R. A. Yund, Studies in diffusion III, oxygen in feldspars: an ion microprobe determination, Geochim. Cosmochim. Acta, 42, 45-57, 1978.

Gooding, J. L., Petrogenetic properties of chondrules in unequilibrated H-, L-, and LL-group chondritic meteorites, Ph.D. thesis, Univ. New Mexico, Albuquerque, 1979.

Gomes, C. B., and K. Keil, Brazilian Stone Meteorites, 162 pp. Univ. New Mexico, Albuquerque, 1980.

Hartmann, W. K., Diverse puzzling asteroids and a possible unified explanation, in Asteroids, edited by T. Gehrels, pp. 466-479, Univ. Arizona Press, Tucson, 1979.

Heiken, G., Petrology of lunar soils, Rev. Geophys. Space Phys., 13, 567-589, 1975.

Hey, M. H., Catalogue of Meteorites, 3rd ed., British Museum (Natural History) London, 1966.

Heyward, T. R., and J. I. Goldstein, Ternary diffusion in the α and γ phases of the Fe-Ni-P system, Metal. Trans., 4, 2335-2342, 1973.

Housen, J. R., L. L. Wilkening, C. R. Chapman, and R. Greenberg, Asteroidal regoliths, Icarus, 39, 317-351, 1979.

Husain, L., ^{40}Ar-^{39}Ar chronology and cosmic ray exposure ages of Apollo 15, samples, J. Geophys. Res., 79, 2588-2606, 1974.

Huss, G. R., The matrix of unequilibrated ordinary chondrites. M.S. thesis, Univ. New Mexico, Albuquerque, 1979.

Huss, G. R., K. Keil, and G. J. Taylor, The matrices of unequilibrated ordinary chondrites: implications for the origin and history of chondrites, Geochim. Cosmochim. Acta, 45, 33-51, 1981.

Hutchison, R., A. W. R. Bevan, and J. M. Hall, Appendix to the Catalogue of Meteorites, British Museum (Natural History), London, 1977.

Jaoul, O., C. Froidevaux, W. B. Durham, and M. Michaut, Oxygen self-diffusion in forsterite: implications for the high-temperature creep mechanism, Earth Planet. Sci. Lett., 47, 391-397, 1980.

Kallemeyn, G. W., W. V. Boynton, J. Willis, and J. T. Wasson, Formation of the Bencubbin polymict meteoritic breccia, Geochim. Cosmochim. Acta, 42, 507-515, 1978.

Keil, K., The electron microprobe X-ray analyzer and its application in mineralogy, Fortschr. Mineral., 44, 4-66, 1967.

Keil, K., Meteorite composition, in Handbook of Geochemistry, edited by K. H. Wedepohl, pp. 78-115, Springer, Heidelberg, 1969.

Keil, K., and R. V. Fodor, Origin and history of the polymict-brecciated Tysnes Island chondrite and its carbonaceous and non-carbonaceous lithic fragments, Chem. Erde, 39, 1-26, 1980.

Keil, K., R. V. Fodor, P. M. Starzyk, R. A. Schmitt, D. D. Bogard, and L. Husain, A 3.6-b.y.-old impact-melt rock fragment in the Plainview chondrite: implications for the age of the H-group chondrite parent body regolith formation, Earth Planet. Sci. Lett., 51, 235-247, 1980.

Kerridge, J. F., and S. W. Kieffer, A constraint on impact theories of chondrule formation, Earth Planet. Sci. Lett., 35, 35-42, 1977.

Konig, H., K. Keil, H. Hintenberger, F. Wlotzka, and F. Begemann, Unterschungen an Steinmeteoriten mit Extrem Hohem Edelgasgehalt. I. Der Chondrit Pantar, Zeitschr. Naturforsch., 16a, 1124-1130, 1961.

Langseth, M. G., S. J. Keihm, and K. Peters, Revised lunar heat-flow values, Proc. Lunar Sci. Conf. 7th, 3143-3171, 1976.

Laul, J. C., and R. A. Schmitt, Chemical composition of Luna 20 rocks and soil and Apollo 16 soils, Geochim. Cosmochim. Acta, 37, 927-942, 1973.

Laul, J. C., and R. A. Schmitt, Chemical composition of Boulder-2 rocks and soils, Apollo 17, Station 2, Earth Planet. Sci. Lett., 23, 206-219, 1974.

Lipschutz, M. E., S. Biswas, and H. Y. McSween, Chemical-petrologic characteristics and origin of gas-rich H-chondrites (abstract), in Lunar and Planetary Science XIII, 439-440, Lunar and Planetary Institute, Houston, 1982.

Martinek, B. J., Evidence for annealing of solar flare tracks in certain gas-rich meteorites (abstract), Meteoritics, 16, 354-355, 1981.

Mason, B., The chemical composition of olivine-bronzite and olivine-hypersthene chondrites, Amer. Mus. Novitates, 2223, 1965.

Mason, B., Handbook of Elemental Abundances in Meteorites,550 pp. Gordon and Breach, New York, 1971.

Mason, B., Cosmochemistry, pt. 1, Meteorites, in Data of Geochemistry, 6th ed., Chapt. B. U.S. Geol. Survey Prof. Pap. 440-B-1, 1979.

Masuda, A., N. Nakamura, and T. Ranaka, Fine structures of mutually normalized rare earth patterns of chondrites, Geochim. Cosmochim. Acta, 37, 239-248, 1973.

McSween, H. Y., Petrographic variations among carbonaceous chondrites of the Vigarano type, Geochim. Cosmochim. Acta, 41, 1777-1790, 1977.

McSween, H. Y., Alteration in CM carbonaceous chondrites inferred from modal and chemical variations in matrix, Geochim. Cosmochim. Acta, 43, 1761-1770, 1979.

McSween, H. Y., and S. M. Richardson, The composition of carbonaceous chondrite matrix, Geochim. Cosmochim. Acta, 41, 1145-1161, 1977.

McSween, H. Y., and M. E. Lipschutz, Origin of volatile-rich H chondrites with light/dark structures, Proc. Lunar Planet. Sci. Conf. 11th, 853-864, 1980.

McSween, H. Y., S. Biswas, and M. E. Lipschutz, Petrogenesis of light and dark portions of the Leighton gas-rich chondritic breccia, Proc. Lunar Planet. Sci. 12B, 1093-1103, 1981.

Nakamura, N., Determination of REE, Fe, Mg, Na and K in carbonaceous and ordinary chondrites. Geochim. Cosmochim. Acta, 38, 757-775, 1974.

Noonan, A. F., and J. A. Nelen, A petrographic and mineral chemistry study of the Weston, Connecticut, chondrite, Meteoritics, 11, 111-130, 1976.

Noonan, A. F., K. Fredriksson, E. Jarosewich, and P. Brenner, Mineralogy and bulk, chondrule, size-fraction chemistry of the Dhajala, India, chondrite (abstract), Meteoritics, 11, 340-343, 1976.

Olsen, E. J., T. K. Mayeda, and R. N. Clayton, Cristobalite-pyroxene in an L6 chondrite: implications for metamorphism, Earth Planet. Sci. Lett., 56, 82-88, 1981.

Onuma, N., R. N. Clayton, and T. K. Mayeda, Oxygen isotope temperatures of 'equilibrated' ordinary chondrites, Geochim. Cosmochim. Acta, 36, 157-168, 1972.

Pellas, P., G. Poupeau, J. C. Lorin, H. Reeves, and J. Audouze, Primitive low-energy particle irradiation of meteoritic crystals, Nature, 223, 272-274, 1969.

Rambaldi, E. R., H. Wanke, and J. W. Larimer, Interelement refractory siderophile fractionation in ordinary chondrites, Proc. Lunar Planet. Sci. Conf. 10th, 997-1010, 1979.

Romig, A. D., Jr., and J. I. Goldstein, Determination of the Fe-Ni and the Fe-Ni-P phase diagrams at low temperatures (700-300°C), Met. Trans., 11A, 1151-1159, 1980.

Rubin, A. E., K. Keil, G. J. Taylor, M.-S. Ma, R. A. Schmitt, and D. D. Bogard, Derivation of a heterogeneous lithic fragment in the Bovedy L-group chondrite from impact-melted porphyritic chondrules, Geochim. Cosmochim. Acta, 45, 2213-2228, 1981.

Rubin, A. E., E. R. D. Scott, and K. Keil, Microchondrule-bearing clast in the Piancaldoli LL3 meteorite: a new kind of type 3 chondrite and its relevance to the history of chondrules, Geochim. Cosmochim. Acta, 46, in press, 1982a.

Rubin A. E., G. J. Taylor, E. R. D. Scott, and K. Keil, Petrologic insights into the fragmentation history of asteroids (abstract) in Workshop on Lunar Breccias and Soils and Their Meteoritic Analogs edited by G. J. Taylor and L. L. Wilkening, pp. 107-110, LPI Tech. Rpt. 82-02, Lunar and Planetary Institute, Houston, 1982b.

Schmitt, R. A., G. G. Goles, R. H. Smith, and T. W. Osborn, Elemental abundances in stone meteorites, Meteoritics, 7, 121-213, 1972.

Scott, E. R. D., Origin of rapidly solidified metal-troilite grains in chondrites and iron meteorites, Geochim. Cosmochim. Acta, 46, 813-823, 1982.

Scott, E. R. D., and R. S. Rajan, Metallic minerals, thermal histories and parent bodies of some xenolithic, ordinary chondrite meteorites. Geochim. Cosmochim. Acta, 45, 53-67, 1981.

Scott, E. R. D., G. J. Taylor, A. E. Rubin, A. Okada, and K. Keil, Graphite-magnetite aggregates in ordinary chondritic meteorites, Nature, 291, 544-546, 1981a.

Scott, E. R. D., A. E. Rubin, G. J. Taylor, and

K. Keil, New kind of type 3 chondrite with a graphite-magnetite matrix, Earth Planet. Sci. Lett., 56, 19-31, 1981b.

Scott, E. R. D., G. J. Taylor, and P. Maggiore, A new LL3 chondrite, Allan Hills A79003, and observations on matrices in ordinary chondrites, Meteoritics, 17, 65-75, 1982.

Sears, D. W., J. N. Grossman, C. L. Melcher, L. M. Ross, and A. A. Mills, Measuring metamorphic history of unequilibrated ordinary chondrites, Nature, 287, 791-795, 1980.

Shima, M., The abundances of titanium, zirconium and hafnium in stony meteorites, Geochim. Cosmochim. Acta, 43, 353-362, 1979.

Smith, B. A., and J. I. Goldstein, The metallic microstructures and thermal histories of severely reheated chondrites, Geochim. Cosmochim. Acta, 41, 1061-1072, 1977.

Smith, B. A., L. Soderblom, R. Batson, P. Bridges, J. Inge, H. Masursky, E. Shoemaker, R. Beebe, J. Boyce, G. Briggs, A. Bunker, S. A. Collins, C. J. Hansen, T. V. Johnson, J. L. Mitchell, R. J. Terrile, A. F. Cook II, J. Cuzzi, J. B. Pollack, G. E. Danielson, A. P. Ingersoll, M. E. Davies, G. E. Hunt, D. Morrison, T. Owen, C. Sagan, J. Veverka, R. Strom, and V. E. Suomi, A new look at the Saturn system: the Voyager 2 images, Science, 215, 504-537, 1982.

Suess, H. E., H. Wanke, and F. Wlotzka, On the origin of gas-rich meteorites, Geochim. Cosmochim. Acta, 28, 595-607, 1964.

Taylor G. J., Petrologic comparison of lunar and meteoritic breccias (abstract) in Workshop on Lunar Breccias and Soils and Their Meteoritic Analogs, edited by G. J. Taylor and L. L. Wilkening, pp. 153-167, LPI Tech. Rpt. 82-02, Lunar and Planetary Institute, Houston, 1982.

Taylor, G. J., and D. Heymann, Postshock thermal histories of reheated chondrites, J. Geophys. Res., 76, 1879-1893, 1971.

Taylor, G. J., K. Keil, J. L. Berkley, D. E. Lange, R. V. Fodor, and R. M. Fruland, The Shaw meteorite: history of a chondrite consisting of impact-melted and metamorphic lithologies, Geochim. Cosmochim. Acta, 43, 323-337, 1979.

Taylor, G. J., E. R. D. Scott, A. E. Rubin, P. Maggiore, and K. Keil, Structure and fragmentation of the parent asteroids of ordinary chondrites (abstract), in Lunar and Planetary Science, XIII, 799-800, Lunar and Planetary Institute, Houston, 1982.

Van Schmus, W. R., Polymict structure of the Mezö-Madaras chondrite, Geochim. Cosmochim. Acta, 31, 2027-2042, 1967.

Wakita, H., R. A. Schmitt, and P. Rey, Elemental abundances of major, minor, and trace elements in Apollo 11 lunar rocks, soil, and core samples, Proc. Apollo 11 Lunar Sci. Conf., 1685-1717, 1970.

Wasson, J. T., Meteorites--Classification and Properties, 316pp. Springer-Verlag, Berlin, 1974.

Wasson, J. T., and G. W. Wetherill, Dynamical, chemical and isotopic evidence regarding the formation locations of asteroids and meteorites, in Asteroids, edited by T. Gehrels, pp. 926-974, Univ. Arizona, Tucson, 1979.

Wetherill, G. W., Future research directions (abstract), in Workshop on Lunar Breccias and Soils and Their Meteoritic Analogs (edited by G. J. Taylor and L. L. Wilkening), p. 17-19, LPI Tech. Rpt. 82-02, Lunar and Planetary Institute, Houston, 1982.

Wilkening, L. L., Foreign inclusions in stony meteorites -- I. carbonaceous chondritic xenoliths in the Kapoeta howardite, Geochim. Cosmochim. Acta, 37, 1985-1989, 1973.

Wilkening, L. L., Meteorites in meteorites: Evidence for mixing among the asteroids, in Comets, Asteroids, Meteorites, edited by A. H. Delsemme, pp. 389-396, Univ. Toledo, Ohio, 1977.

Willis, J., and J. I. Goldstein, A revision of metallographic cooling rate curves for chondrites, Proc. Lunar Planet. Sci., 12B, 1135-1143, 1981.

Wood, J. A., Chondrites: their metallic minerals, thermal histories, and parent planets, Icarus, 6, 1-49, 1967.

(Received April 30, 1982;
revised July 19, 1982
accepted September 1, 1982.)